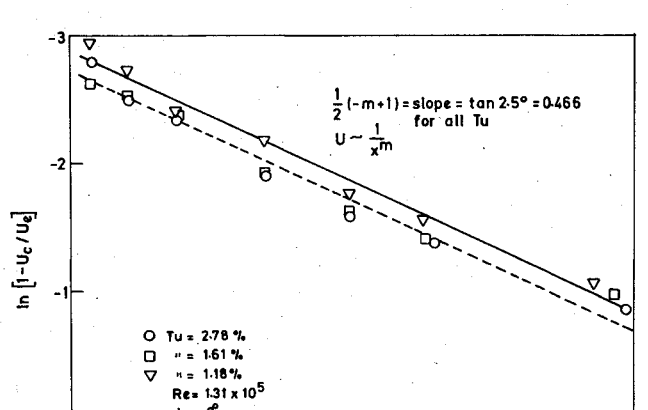

Fig. 3 Variation of wake centerline velocity with downstream distance.

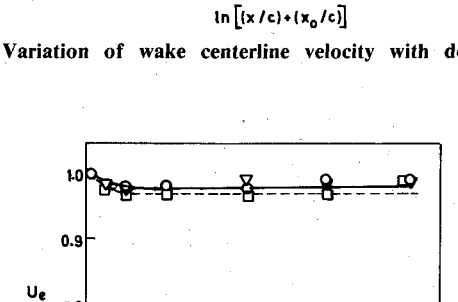

Fig. 4 Variation of wake edge velocity with downstream distance.

pronounced. The velocity distribution tends to become uniform faster at higher values of Tu.

Using scaling velocity as the difference between the maximum and minimum velocity $(U_e - U_c)$, and two different scaling lengths L_{0s} and L_{0p} (Ref. 5) for suction and pressure sides, respectively, the mean velocity distribution shows similarity at various values of x/c. The similarity curves for a 12-deg incidence angle are shown in Fig. 2. L_{0s} and L_{0p} are respectively the distances on the suction and pressure sides of the wake centerline, from the point of minimum velocity to a point where velocity is $\frac{1}{2}(U_e - U_c)$. Figure 3 shows the variation of wake centerline velocity with downstream distance on a logarithmic scale. x_0/c (the virtual origin) has been obtained using the method of Ref. 5. Its values range from 0.019 to 0.032. x_0/c is observed to decrease with an increase in Tu. The ratio of centerline velocity to wake edge velocity increases with freestream turbulence in the far wake. Figure 4 presents the variation of wake edge velocity with downstream distance. The velocity is nearly constant in the far wake.

The calculations for the drag coefficient C_d show that it decreases slightly with an increase in Tu. The values of C_d for three turbulence intensities of 1.18, 1.61, and 2.78% are respectively 0.013, 0.011, and 0.011 at an incidence angle of 12 deg. The value of the drag coefficient in Ref. 2 (for a solidity of 1.25) is 0.0170. The freestream turbulence may play a role in delaying separation in a low Reynolds number flow and this is likely to reduce C_d. Emery et al.[2] have also noted a decrease in drag coefficient when freestream turbulence was increased by placing a grid before the test section.

Conclusions

Experimental investigations have been carried out to determine the characteristics of a compressor cascade wake at three different values of freestream turbulence levels. The results indicate that the wake decay is faster for the case of higher freestream turbulence levels. A slight decrease in drag coefficient was also observed as the turbulence level was increased. The present investigations were limited to $Tu = 2.78\%$. At higher values of Tu these effects are expected to be more pronounced.

Similarity in the velocity distribution is observed in the near wake and far wake regions at all three values of incidence and turbulence levels.

References

[1] Schlichting, H. and Das, A., "On the Influence of Turbulence Level on the Aerodynamic Losses of Axial Turbomachines," *Symposium on Flow Research on Blading*, edited by L.S. Dzung, Elsevier, New York, 1970, pp. 243-274.

[2] Emery, C.J., Herring, L.J., Erwin, J.R., and Felix, A.R., "Systematic Two-Dimensional Tests of NACA 65-Series Compressor Blades at Low Speeds," NACA Report 1368, 1958.

[3] Evans, R.L., "Freestream Turbulence Effects on the Turbulent Boundary Layer," Aeronautical Research Council C.P. 1282, 1974.

[4] Citavy, J. and Norbury, J.F., "The Effect of Reynolds Number and Turbulence Intensity on the Performance of a Compressor Cascade with Prescribed Velocity Distribution (PVD)," *Journal of Mechanical Engineering Science*, Vol. 19, No. 3, 1977, pp. 93-100.

[5] Raj, R. and Lakshminarayana, B., "Characteristics of the Wake Behind a Cascade of Airfoils," *Journal of Fluid Mechanics*, Vol. 61, Dec. 1977, pp. 707-730.

[6] Gustafson, W.A. and Davis, D.W., "Analysis of the Turbulent Wake of a Cascade Airfoil," *Journal of Aircraft*, Vol. 14, April 1977, pp. 350-356.

[7] Felix, R.A. and Emery, J.C., "A Comparison of Typical National Gas Turbine Establishment and NACA Axial Flow Compressor Blade Sections in Cascade at Low Speed," NACA TN 3937, 1957.

[8] Nowack, C.F.R., "Improved Calibration Method for Five-Hole Spherical Pitot Probe," *Journal of Physics E*, Vol. 3, No. 1, 1970, pp. 22-26.

The Effect of Displacement Velocity on Propeller Performance

Michio Nishida*
Kyoto University, Kyoto, Japan

In Refs. 1 and 2, simple vortex lattice methods were applied to propeller performance analysis. The propeller blade used in these papers is such that a single bound vortex is placed at the quarter-chord and a helical trailing vortex leaves both sides of each radial section on the quarter-chord line. The vortex method is to find the induced velocity due to the bound and helical vortices at the control points located on the three-quarter chord of each radial section by using the condition of no normal velocity to the surface. The analysis needs the position of the helical vortex. In Refs. 1 and 2 it is assumed that the helical trailing vortex leaves the blade at a freestream velocity V_∞. However, it is reasonable to consider that the trailing vortex moves with a velocity $V_\infty + \frac{1}{2}W$, where W is the axial displacement velocity at infinity. The purpose of this Note is to investigate the contribution of the displacement velocity to propeller performance.

At the control points the velocity normal to the blade surface must vanish:

$$V \cdot n = 0 \tag{1}$$

Received Sept. 17, 1982.

*Associate Professor, Department of Aeronautical Engineering.

where V is the induced velocity plus the freestream velocity and n is the normal vector on the blade surface. The components of the induced velocity in the x, y, and z directions at the jth control point are expressed as

$$\begin{bmatrix} u_j/V_\infty \\ v_j/V_\infty \\ w_j/V_\infty \end{bmatrix} = \sum_{i=1}^{M} \frac{\Gamma_i}{4\pi R V_\infty} \begin{bmatrix} FU_{ij} \\ FV_{ij} \\ FW_{ij} \end{bmatrix} \tag{2}$$

where R is the blade radius, Γ_i the circulation in the ith radial section, M the number of the radial section, and FU_{ij}, FV_{ij}, and FW_{ij} are the influence coefficients. Substituting the obtained induced velocities into Eq. (1), we have[2]

$$\sum_{i=1}^{M} \frac{\Gamma_i}{4\pi R V_\infty} [FU_{ij}(f_x)_j + FV_{ij}(f_y)_j - FW_{ij}]$$
$$= \frac{\omega r_j \sin\psi_j}{V_\infty}(f_x)_j - \frac{\omega r_j \cos\psi_j}{V_\infty}(f_y)_j + 1 \tag{3}$$

where f_x and f_y are such that $n = -f_x i - f_y j + k$, and ω is the angular velocity of the propeller. We have let the control point be on a position (r, ψ, z_c). Equation (3) forms M linear equations. Once we obtain Γ_i from Eq. (3), the induced velocities can easily be determined from Eq. (2).

The influence coefficients are written as[2]

$$\begin{bmatrix} FU_{ij} \\ FV_{ij} \\ FW_{ij} \end{bmatrix} = \begin{bmatrix} FUH_{i+1,1} \\ FVH_{i+1,1} \\ FWH_{i+1,1} \end{bmatrix} - \begin{bmatrix} FUH_{ij} \\ FVH_{ij} \\ FWH_{ij} \end{bmatrix} + \begin{bmatrix} FUB_{ij} \\ FVB_{ij} \\ FWB_{ij} \end{bmatrix} \tag{4}$$

where FUH, FVH, and FWH are the influence coefficients due to the helical vortex, and FUB, FVB, and FWB are the influence coefficients due to the bound vortex which are given in Ref. 2.

Although the expressions for FUH, FVH, and FWH are also given in Ref. 2, we must make slight corrections for the expressions. A position on a helical trailing vortex line which leaves a position on the one-quarter chord (r_v, θ_0, z_0) is defined by

$$x_v = r_v\cos\theta, \quad y_v = r_v\sin\theta, \quad z_v = \frac{V_\infty + \frac{1}{2}W}{\omega R}(\theta - \theta_0) + z_0 \tag{5}$$

where x_v, y_v, z_v, r_v, and z_0 are nondimensionalized with respect to the blade radius R. The influence coefficients due to a helical trailing vortex line having strength of circulation per length Γ are expressed as

$$\begin{bmatrix} FUH \\ FVH \\ FWH \end{bmatrix} = \int \frac{d\theta}{d^3} \begin{bmatrix} r_v\cos\theta\left[z_c - z_0 - \frac{V_\infty}{\omega R}\left(1 + \frac{1}{2}\frac{W}{V_\infty}\right)(\theta - \theta_0)\right] \\ \quad - \frac{V_\infty}{\omega R}\left(1 + \frac{1}{2}\frac{W}{V_\infty}\right)(r\sin\psi - r_v\sin\theta) \\ r_v\sin\theta\left[z_c - z_0 - \frac{V_\infty}{\omega R}\left(1 + \frac{1}{2}\frac{W}{V_\infty}\right)(\theta - \theta_0)\right] \\ \quad + \frac{V_\infty}{\omega R}\left(1 + \frac{1}{2}\frac{W}{V_\infty}\right)(r\cos\psi - r_v\cos\theta) \\ r_v^2 - r_v r\cos(\theta - \psi) \end{bmatrix} \tag{6}$$

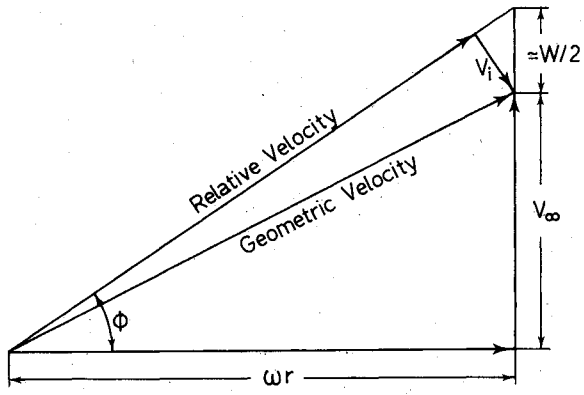

Fig. 1 Velocity diagram.

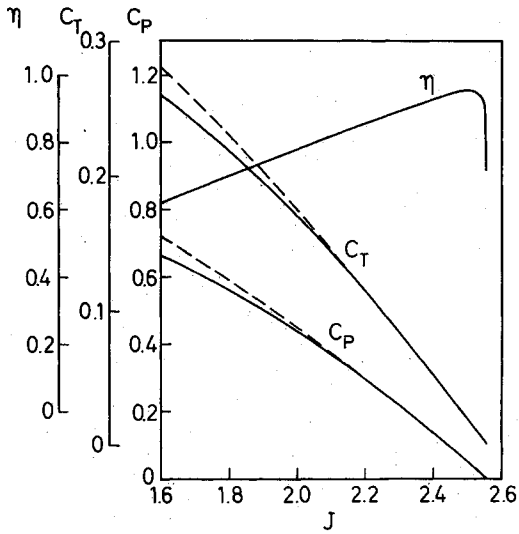

Fig. 2 Calculated propeller characteristics, $\beta_{3/4} = 47.5$ deg. Solid curve: displacement velocity considered; chained curve: displacement velocity not considered.

where

$$d = \begin{bmatrix} r\cos\psi - r_v\cos\theta \\ r\sin\psi - r_v\sin\theta \\ z_c - \frac{V_\infty}{\omega R}\left(1 + \frac{1}{2}\frac{W}{V_\infty}\right)(\theta - \theta_0) - z_0 \end{bmatrix} \tag{7}$$

The displacement velocity W appearing in Eq. (5) is unknown, hence we must estimate it from the velocity diagram shown in Fig. 1. From this figure we can easily deduce the following:

$$W = 2V_i/\cos\phi \tag{8}$$

where $V_i = (v^2 + \omega^2)^{1/2}$. Also we have

$$\tan\phi = \frac{V_\infty + \frac{1}{2}W}{\omega R}\frac{1}{r} = \frac{V}{\omega R}\left(1 + \frac{1}{2}\frac{W}{V_\infty}\right)\frac{1}{r} \tag{9}$$

By employing ϕ from Eq. (9) in Eq. (8), the displacement velocity W is determined.

Let the initial value of W be zero in Eqs. (5) and (6). We can then determine the local circulation Γ from Eq. (3) and hence the induced velocity from Eq. (2). After determining induced velocity, the displacement velocity can be evaluated by using Eqs. (8) and (9). When we use the newly determined value of W in Eqs. (5) and (6), the value of Γ is renewed. Thus an iterative scheme is continued until the value of the induced velocity converges.

Numerical calculations were made for the 54H60 propeller developed by Hamilton Standard. The thrust coefficient C_T, the power coefficient C_P, and the propeller efficiency η vs the advance ratio J are shown in Fig. 2. C_T and C_P are lower when the displacement velocity is taken into account than when it is not considered. This is because in the former case the helical trailing vortex leaves the blade more rapidly than in the latter case. Hence the pitch of the helical vortex becomes larger in the first case, which leads to the fact that the velocity induced by the helical vortex is weak. The difference between the results for both cases decreases with increasing advance ratio. A large advance ratio corresponds to a lightly loaded propeller, so that the contribution of the displacement velocity reasonably becomes small for such a lightly loaded propeller.

As shown in Fig. 2, the difference between the propeller efficiencies for both cases is negligible.

The numerical calculations showed that only three or four iterations were needed for the induced velocities to be converged.

References

[1]Baskin, V.E., Vil'dgrube, L.S., Vozhdayev, Ye. S. and Maykapar, G.I., "The Theory of the Lifting Airscrew," NASA TT-F-823, 1973.

[2]Sullivan, J.P., "The Effect of Blade Sweep on Propeller Performance," AIAA Paper 77-716, June 1977.